Title: **The role of p21-activated kinases (PAKs) in glucose homeostasis and skeletal muscle glucose uptake**

Lisbeth L. V. Møller[1], Merna Jaurji[1], Ida L. Nielsen[1], Rasmus Kjøbsted[1], Giselle A. Joseph[2], Agnete B. Madsen[1], Jonas R. Knudsen[1], Peter Schjerling[3,4], Thomas E. Jensen[1], Robert S. Krauss[2], Erik A. Richter[1*], and Lykke Sylow[1*]

[1] Section of Molecular Physiology, Department of Nutrition, Exercise and Sports, Faculty of Science, Section of Molecular physiology, University of Copenhagen, Denmark

[2] Department of Cell, Developmental, and Regenerative Biology, Icahn School of Medicine at Mount Sinai, New York, NY 10029 USA

[3] Institute of Sports Medicine, Department of Orthopedic Surgery, Bispebjerg Hospital, Denmark

[4] Center for Healthy Aging, Faculty of Health Sciences, University of Copenhagen, Denmark

[*]*Corresponding authors and persons to who reprint requests should be addressed. Authors contributed equally.*

Lykke Sylow, Lshansen@nexs.ku.dk, phone +4520955250

Erik Arne Richter, Erichter@nexs.ku.dk, phone +4528751626

Universitetsparken 13, 2100 Copenhagen OE, Denmark

Number of figures: 7 (+ 2 supplemental figures)

Abstract:

Skeletal muscle glucose transport is essential for maintaining whole body glucose homeostasis and skeletal muscle accounts for the majority of glucose disposal in response to insulin. Glucose transport into skeletal muscle can be induced by several stimuli, such as insulin and muscle contraction, which both have been shown to activate group I p21-activated kinases (PAKs).

Skeletal muscle expresses two group I PAK isoforms but the role of these in muscle glucose uptake has not been determined. Recent evidence suggests that p21-activated kinase (PAK) 1 may play a role in insulin-stimulated GLUT4 translocation and that PAK1/2 signaling is markedly impaired in insulin resistant skeletal muscle. Thus, the current study aimed to test the hypothesis that PAKs are important regulators of glucose homeostasis and skeletal muscle glucose uptake.

To elucidate the role for group I PAKs in skeletal muscle glucose uptake, we determined glucose uptake in mature skeletal muscle incubated with a pharmacological inhibitor of group I PAKs, IPA-3, or in mice with knockout (KO) of either PAK1, PAK2, or joint KO of both PAK1 and PAK2 (d1/2KO). In contrast to our hypothesis, we found that lack of PAK1 did not affect glucose uptake in response to insulin or contraction. Lack of PAK2 protein only mildly reduced insulin-stimulated glucose transport in EDL muscle. We conclude that PAK1/2 proteins are not major regulators of skeletal muscle glucose uptake but that PAK2 may play a minor role.

Introduction

Skeletal muscle is a major glucose sink for disposal and storage of excessive glucose from the blood and is therefore essential in maintaining whole body glucose homeostasis. Skeletal muscle obtains this function by increasing glucose uptake in response to insulin during conditions of high blood glucose. Understanding the mechanisms regulating glucose uptake by skeletal muscle is important because muscle accounts for most insulin-mediated glucose disposal (1) and is relevant in the pathophysiology of insulin resistance and type 2 diabetes mellitus (1,2).

Insulin facilitates glucose transport in skeletal muscle by activation of a signaling cascade that lead to the translocation of glucose transporter GLUT4 containing vesicles to the sarcolemma and transverse tubuli (3). This signaling cascade includes activation of phosphoinositide 3-kinase (PI3K) and Akt that regulate GLUT4 translocation via phosphorylation of TBC1D4 and Rab proteins (4,5). Another important, although not as well described regulator of GLUT4 translocation in muscle cells is Rac1 (6–8). We and others have shown that glucose transport in response to insulin, contraction and passive stretching partially rely on Rac1 (9–12) but the downstream mechanisms remain unknown.

The kinase, PAK1 was discovered as a binding partner and target of Rac in the rat brain in 1994 (13). PAK1 together with two other kinases, PAK2 and PAK3, constitute the group I PAKs. Group I PAKs have been extensively studied as part of numerous signaling networks that regulate essential cellular activities, including cell proliferation, differentiation, apoptosis, and cytoskeleton dynamics (14,15). In skeletal muscle only PAK1 and PAK2 are expressed (16).

In 1996 in L6 myotubes, PAK1 was found to be phosphorylated in response to insulin stimulation downstream of PI3K (17). Interestingly, treating cultured muscle cells with glucose oxidase, which

mimics insulin resistance *in vitro*, led to inhibition of the upstream target of PAK1/2, Rac1 (7), and even though Rac1-GTP binding was not impaired in palmitate treated insulin resistant L6 myotubes, insulin-stimulated PAK1/2 phosphorylation of threonine 423/402 was diminished (18). Furthermore, insulin-induced pPAK1/2 T423/402 phosphorylation was 50% reduced in muscle from subjects with obesity and type 2 diabetes (9). A pharmacological inhibitor of group I PAKs, IPA-3 abolished insulin-stimulated GLUT4 translocation and glucose uptake into L6 myoblasts and myotubes, respectively (16) suggesting that PAKs are involved in glucose uptake regulation. Indeed, whole body genetic ablation of PAK1 in mice lead to mildly impaired glucose tolerance (19,20). This was associated with defects in GLUT4 translocation in skeletal muscle as well as reduced insulin production in pancreatic beta cells (19).

Although such studies point towards a role for group I PAKs, and particular PAK1 in regulation of glucose homeostasis and transport into skeletal muscle, a systematic analysis of the involvement of group I PAKs in the regulation of glucose transport in skeletal muscle has not yet been undertaken and thus is warranted. Here, we performed a systematic series of genetic and pharmacologic experiments to investigate the involvement of group I PAKs. We hypothesized that PAKs, and in particular PAK1, would play a major role in glucose transport in response to insulin and contraction. In contrast to our hypothesis, we found that PAK2, but not PAK1, is partially involved in glucose transport in skeletal muscle.

Methods

Animals. Female C57BL/6J mice (Taconic, Denmark) were used for all inhibitor incubation studies. Mice received standard rodent chow diet (Altromin no. 1324; Brogaarden, Denmark) and water ad libitum.

Whole-body PAK1$^{-/-}$ mice. Whole-body PAK1$^{-/-}$ mice on a C57BL/6J background were generated as previously described (21). Mice were obtained by heterozygous crossing. PAK1$^{-/-}$ mice (hereafter referred to as PAK1 knockout (KO)) and paired littermate PAK1$^{+/+}$ mice (hereafter referred to as controls) were used for experiments. Female and male mice 12-24 weeks of age were used for measurement of *in vitro* insulin-stimulated glucose transport in isolated muscle. Number of mice in each group: Control, *n = 6/7* (female/male); PAK1 KO, *n = 4/8*. Female and male mice 7-13 weeks of age were used for measurement of *in vitro* contraction-stimulated glucose transport in isolated muscle. Number of mice in each group: Control, *n = 10/2* (female/male); PAK1 KO, *n = 8/2*. Mice received standard rodent chow diet (Altromin no. 1324; Brogaarden, Denmark) and water ad libitum.

For measurement of *in vivo* insulin-stimulated glucose uptake in chow or 60E% high-fat diet (HFD 60E%; no. D12492; Brogaarden, Denmark) fed PAK1 KO mice, mice were assigned to a chow or HFD 60E% group. Chow fed mice were terminated at 10-24 weeks of age. Number of mice in each group: Control-Chow, *n = 14/8* (female/male); PAK1 KO-Chow, *n = 6/4*. For mice receiving HFD 60E%, the intervention started at 6-16 weeks of age and lasted for 21 weeks. Mice were terminated at 27-37 weeks of age. Number of mice in each group: Control-HFD 60E%, *n = 7/7* (female/male); PAK1 KO-HFD 60E%, *n = 11/5*. Mice had access to their respective diet and water ad libitum.

Double PAK1$^{-/-}$;PAK2$^{fl/fl}$;MyoD$^{iCre/+}$ mice. Double knockout mice with whole-body knockout of PAK1 and conditional, muscle-specific knockout of PAK2, PAK1$^{-/-}$;PAK2$^{fl/fl}$;MyoD$^{iCre/+}$ were generated as previously described (14). Mice were on a mixed C57BL/6/FVB background. PAK1$^{-/-}$;PAK2$^{fl/fl}$;MyoD$^{iCre/+}$ (hereafter referred to as d1/2KO) were crossed with PAK1$^{+/-}$;PAK2$^{fl/fl}$;MyoD$^{+/+}$ (hereafter referred to as controls) to generate d1/2KO, PAK1$^{-/-}$;PAK2$^{fl/fl}$;MyoD$^{+/+}$ (hereafter referred to as PAK1 KO), PAK1$^{+/-}$;PAK2$^{fl/fl}$;MyoD$^{iCre/+}$ (hereafter referred to as PAK2 mKO), and paired littermate controls used for experiments. Female and male

mice 10-16 weeks of age were used for measurement of *in vitro* insulin-stimulated glucose transport in isolated muscle. Number of mice in each group: Control, *n = 6/4* (female/male); PAK1 KO, *n = 5/4*, PAK2 mKO, *n = 6/4*, d1/2KO, *n = 6/3*. Mice received standard rodent chow diet (Altromin no. 1324; Brogaarden, Denmark) and water ad libitum.

All animals were maintained on a 12:12 hour light-dark cycle and housed at 22±2°C with nesting material. Mice were group housed. All experiments were approved by the Danish Animal Experimental Inspectorate.

Body composition. Body composition was analyzed using magnetic resonance imaging (EchoMRI-4in1TM, Echo Medical System LLC, Texas, USA). Chow fed PAK1 KO or control littermates were assessed at 7-19 weeks of age. HFD 60E% fed PAK1 KO or control littermates were assessed 18 weeks into the diet intervention (24-34 weeks of age). Fat mass (FM) and lean body mass (LBM) were related to total body mass (BM).

Glucose tolerance test (GTT). Mice were fasted for 12 hours from 10 p.m. D-mono-glucose (2 g kg^{-1} body weight) was administered intraperitoneal (i.p) and blood was collected from the tail vein and blood glucose concentration determined using a glucometer (Bayer Contour, Bayer, Switzerland). Blood glucose concentration was determined at time points 0, 20, 40, 60, 90, and 120 minutes in chow fed PAK1 KO mice or littermate controls (8-20 weeks of age). Glucose tolerance was assessed 14 weeks into the diet intervention in HFD 60E% fed PAK1 KO mice or littermate controls (20-30 weeks of age), and blood glucose concentration was determined at time points 0, 30, 60, 90, and 120. For measurements of plasma insulin, glucose was administered i.p. and blood was sampled at time points 0 and 20 minutes, centrifuged and plasma was quickly frozen in liquid

nitrogen and stored at -80°C until processing. Plasma insulin was analyzed in duplicate (Mouse Ultrasensitive Insulin ELISA, #80-INSTRU-E10, ALPCO Diagnostics, USA).

In vitro incubation of isolated muscle. Soleus and extensor digitorum longus (EDL) muscles were dissected from anaesthetized female C57BL/6J mice or male and female PAK1 KO, PAK2 mKO, d1/2KO mice or control littermates (6 mg pentobarbital sodium 100 g^{-1} body weight i.p.) and suspended at resting tension (4-5 mN) in incubations chambers (Multi Myograph System, Danish Myo Technology, Denmark) in Krebs-Ringer-Henseleit (KRH) buffer with 2 mM pyruvate and 8 mM mannitol at 30°C, as described previously (22). Additionally, the KRH buffer was supplemented with 0.1% BSA (v/v) during experiments with electrically-induced contractions. For inhibitor experiments, the muscles were incubated for a total of time of 55-60 minutes in KRH buffer with IPA-3 (40 µM, SigmaAldrich) or a corresponding amount of DMSO as vehicle control. The incubation chambers were kept dark to avoid degradation of light-sensitive compounds. Before 30 minutes of insulin-stimulation (60 nM; Actrapid, Novo Nordisk, Denmark), muscles were pre-incubated for 25 minutes. Before 15 minutes of electrically-stimulated contraction, muscles were pre-incubated for 45 minutes. Contractions were induced by electrical stimulation every 15 sec with 2-sec trains of 0.2 msec pulses delivered at 100 Hz (~35V) for 15 minutes. PAK1 KO or littermate controls were pre-incubated in KRH buffer for 30 minutes. After pre-incubation, muscles were stimulated with insulin for 30 minutes (6 nM or 60 nM) or electrically-stimulated to contract. PAK1 KO, PAK2 mKO, d1/2 KO mice or control littermates were pre-incubated for 15-20 minutes followed by 20 minutes of insulin stimulation (60 nM).

2 Deoxy-glucose (2DG) transport was measured with 1 mM 2DG during the last 10 min of the stimulation period using 0.75 µCi mL^{-1} [^{3}H]2DG and 0.225 µCi mL^{-1} [^{14}C]mannitol radioactive tracers as described previously (22).

In vivo insulin-stimulated 2 Deoxy-glucose uptake in PAK1 KO mice. To determine 2 Deoxy-glucose (2DG) uptake in skeletal muscle of PAK1 KO mice or littermate controls, [3H]2DG (Perkin Elmer) was injected retro-orbitally (r.o.) in a bolus of saline containing 66.7 μCi mL^{-1} [^{3}H]2DG corresponding to ~10 μCi/mouse in chow fed mice or ~15 μCi/mouse in HFD 60E% fed mice (6 μL g^{-1} body weight). The [^{3}H]2DG saline bolus also contained insulin (Actrapid, Novo Nordisk, Denmark) or a comparable volume of saline. Decreased insulin clearance has been observed by us (23) and others in obese rodent (24,25) and human (26) models. Therefore to correct for changes in insulin clearance, 0.5 U kg^{-1} body weight of insulin was administered in chow mice whereas only 60% of this dosage was administered to HFD 60E% mice. Prior to stimulation, mice were fasted for 4 hours from 07:00 and anaesthetized (i.p. injection of 7.5/9 mg (Chow/HFD 60E%) pentobarbital sodium 100 g^{-1} body weight) 15 minutes before the r.o. injection. Blood samples were collected from the tail vein prior to and 5 and 10 minutes after the r.o. injection and analyzed for glucose concentration using a glucometer (Bayer Contour, Bayer, Switzerland). After 10 minutes, skeletal muscle (gastrocnemius, quadriceps, and triceps brachii) were excised, quickly frozen in liquid nitrogen and stored at -80°C until processing. Blood was collected by punctuation of the heart, centrifuged and plasma was quickly frozen in liquid nitrogen and stored at -80°C until processing. Plasma samples were analyzed for insulin concentration and specific [^{3}H]2DG tracer activity. Plasma insulin was analyzed in duplicate (Mouse Ultrasensitive Insulin ELISA, #80-INSTRU-E10, ALPCO Diagnostics, USA). Tissue specific 2DG-6-phosphate accumulation was measured as described (27,28). The tissue specific [^{3}H]2DG-6-P was divided by area under the curve (AUC) of the specific [^{3}H]2DG tracer activity in the plasma for time points 0 and 10 minutes to determine 2DG clearance from the plasma into the specific tissue. To estimate tissue-specific 2DG uptake, clearance was multiplied by the average blood glucose levels for the time points 0, 5, and 10 minutes. Tissue specific 2DG clearance and 2DG uptake were related to tissue weight and time.

Muscle analyses. Gastrocnemius, quadriceps, and triceps muscles were pulverized in liquid nitrogen. All muscle were homogenized 2 x 30 sec at 30 Hz using a Tissuelyser II (Qiagen, USA) in ice-cold homogenization buffer (10% (v/v) Glycerol, 1% (v/v) NP-40, 20 mM Na-pyrophosphate, 150 mM NaCl, 50 mM HEPES (pH 7.5), 20 mM β-glycerophosphate, 10 mM NaF, 2mM PMSF, 1 mM EDTA (pH 8.0), 1 mM EGTA (pH 8.0), 2 mM Na3VO4, 10 µg mL^{-1} Leupeptin, 10 µg mL^{-1} Aprotinin, 3 mM Benzamidine). After rotation end-over-end for 30 min at 4°C, lysate supernatants were collected by centrifugation (10,000 x g) for 15-20 min at 4°C.

Immunoblotting. Lysate protein concentration was determined using the bichinchoninic acid (BCA) method using BSA standards and BCA assay reagents (Pierce). Immunoblotting samples were prepared in 6x sample buffer (340 mM Tris (pH 6.8), 225 mM DTT, 11% (w/v) SDS, 20% (v/v) Glycerol, 0.05% (w/v) Bromphenol blue). Protein phosphorylation (p) and total protein expression were determined by standard immunoblotting technique loading equal amounts of protein. The polyvinylidene difluoride membrane (Immobilon Transfer Membrane; Millipore) was blocked in Tris-Buffered Saline with added Tween20 (TBST) 2% (w/v) skim milk or 5% (w/v) BSA protein for 15 minutes at room temperature, followed by incubation overnight at 4°C with the primary antibody (Table 1). Next, the membrane was incubated with horseradish peroxidase-conjugated secondary antibody (Jackson Immuno Research) for 1 hour at room temperature. Bands were visualized using Bio-Rad ChemiDocTM MP Imaging System and enhanced chemiluminescence (ECL+; Amersham Biosciences). Densitometric analysis was performed using Image LabTM Software, version 4.0 (Bio-Rad, USA). Total actin protein expression or coomassie brilliant blue staining was used as a loading control (29).

Statistical analyses. Results are presented as mean ± S.E.M. or when feasible mean ± S.E.M. with individual values shown. Initial force development from inhibitor and PAK1 KO studies and body composition in PAK1 KO mice and littermate controls were evaluated using t-tests. Body mass at

experimental day and energy intake of PAK1 KO mice and littermate controls were evaluated using a two-way ANOVA. *In vitro* 2DG transport and signaling data from inhibitor and PAK1 KO studies and GTT blood glucose and plasma insulin in PAK1 KO and littermate controls were evaluated using a two-way repeated-measures (RM) ANOVA.

For the blood glucose curve during the ITT in the PAK1 KO HFD 60E% study, two two-way RM ANOVAs were applied; one two-way RM ANOVA was used to test the factors 'time' (0 vs. 5 vs. 10 minutes) and 'genotype' (control vs. PAK1 KO) in chow fed mice alone. Similarly, a second two-way RM ANOVA was used to test the factors 'time' and 'genotype' in HFD 60E% fed mice alone. Additionally, three two-way ANOVAs were applied to test the factors 'genotype' and 'diet' at time point 0, 5, and 10 minutes, respectively. For 2DG uptake and 2DG clearance, four two-way ANOVAs were applied: two two-way ANOVAs were used to test the factors 'stimuli' (basal vs. insulin) and 'genotype' (control vs. PAK1 KO) in chow and HFD 60E% fed mice, separately. Additionally, two two-way ANOVAs were applied to test the factors 'genotype' and 'diet' in the basal and insulin-stimulated state, respectively.

For 2DG transport and signaling in the PAK1/2 dKO study, four two-way RM ANOVAs were applied; one two-way RM ANOVA was used to test the factors 'stimuli' (basal vs. insulin) and 'PAK1' ($PAK1^{+/-}$ vs. $PAK^{-/-}$) for the $PAK2^{fl/fl}$;$MyoD^{+/+}$ alone. Similarly, a second two-way RM ANOVA was used to test the factors 'stimuli' and 'PAK1' for $PAK2^{fl/fl}$;$MyoD^{iCre/+}$ mice alone. A third and fourth two-way RM ANOVA tested the factors 'stimuli' and 'PAK2' ($PAK2^{fl/fl}$;$MyoD^{+/+}$ vs. $PAK2^{fl/fl}$;$MyoD^{iCre/+}$) for $PAK1^{+/-}$ and $PAK^{-/-}$ mice, separately. Additionally, two two-way ANOVAs were applied to test the factors 'PAK1' and 'PAK2' in the basal and insulin-stimulated state, respectively. For total protein expression (average of paired basal and insulin-stimulated samples) from PAK1/2 dKO studies, a two-way ANOVA was applied to test the factors 'PAK1' and 'PAK2'.

If the null hypothesis was rejected, Tukey's post hoc test was used to evaluate main effects and significant interactions in ANOVAs. $P < 0.05$ was considered statistically significant. $P<0.1$ was considered a tendency. All statistical analyses were performed using Sigma Plot, version 13 (Systat Software Inc., Chicago, IL, USA).

Results

Pharmacological inhibition of group I p21-activated kinases partially reduces insulin-stimulated glucose transport in mouse soleus muscle. Skeletal muscle expresses both p21-activated kinase (PAK)1 and PAK2, but not the PAK3 isoform (16). IPA-3 is a well characterized inhibitor of group I PAKs (PAK1-3) (16,30) and is expected to inhibit both PAK1 and PAK2 at the applied concentration. To test the involvement of PAK1/2 in insulin-stimulated glucose uptake, we analyzed 2 deoxy-glucose (2DG) transport in isolated soleus and extensor digitorum (EDL) muscles stimulated with 60 nM insulin, a dose that maximally stimulates glucose transport *in vitro* (31). In soleus, insulin-stimulation increased 2DG transport 4.5-fold and this increase was reduced (-20%) in IPA-3-treated muscles (Figure 1A). IPA-3 did not significantly impair insulin-stimulated 2DG transport in EDL muscle (Figure 1B). In contrast to the relatively modest effect in our incubated muscles, IPA-3 has previously been reported to completely abolish insulin-stimulated GLUT4 translocation and glucose transport into L6 myoblasts and myotubes, respectively (16). We confirmed that IPA-3 treatment completely abolished insulin-stimulated Threonine 423 (activation site) phosphorylation of PAK1 (pPAK1 T423) in both soleus and EDL muscle (Figure 1C+D) with no effects on pAkt S473 (Figure 1E+F) or pAkt T308 (Figure 1G+H). Thus, PAK1/2 seem to be only partially involved in insulin-stimulated glucose transport in isolated mouse muscle. Also, inhibition of PAK1/2 does not interfere with insulin signaling to Akt suggesting that PAKs are not upstream regulators of Akt in response to insulin.

Contraction-stimulated glucose transport is partially inhibited by pharmacological inhibition of PAK1/2. Because the upstream activator of PAK1/2, Rac1 is also involved in contraction-stimulated glucose transport, we newt sought to investigate whether Rac1 may regulate glucose transport through its activation of PAK1/2. In control DMSO-treated muscle, electrically-induced contraction stimulated a 3-fold increase in 2DG transport in soleus and EDL muscle (Figure 2A+B). IPA-3 partly inhibited (-22%) this increase in 2DG transport in both muscles (Figure 2A+B). This reduction in 2DG transport in IPA-3-treated soleus and EDL muscle, was not associated with reduced initial force development by IPA-3 treated muscles (Figure 2C).

It is unknown if PAK1/2 may regulate 5' AMP-activated protein kinase (AMPK), a metabolic sensor highly activated during muscle contraction and a regulator of glucose uptake (32,33). Pharmacological inhibition of group I PAKs did not affect pAMPK T172 in soleus muscle (Figure 2D). However, contraction-stimulated pAMPK T172 was reduced (-46%) in IPA-3-treated EDL muscle (Figure 2E) implying that PAK1 and/or PAK2 participate in contraction-induced activation of AMPK in highly glycolytic muscles, such as EDL. However, AMPKs downstream target pACC2 S212 was normally phosphorylated in response to contraction in both muscles (Figure 2F+G). This shows for the first time, that IPA-3 partially inhibits contraction-stimulated glucose uptake in skeletal muscle.

PAK1 knockout does not affect whole body glucose tolerance or insulin-stimulated 2DG transport in isolated skeletal muscle. Pharmacological inhibitors often have unknown off target effects and we therefore next sought to confirm our findings in mice lacking the PAK1 isoform. Previously, these mice have been shown to display abolished GLUT4 translocation in response to insulin (19). Body composition (Figure 3A-B) and body mass (Figure 3A) was similar in chow fed PAK1 knockout (KO) mice and control littermates as also reported previously (20). Moreover, the lack of PAK1 had no effect on whole body glucose tolerance (Figure 3C). Also, the plasma insulin

concentration increased to a similar extent in response to glucose administration during the GTT in PAK1 KO mice compared to littermate control (Figure 3D). Furthermore, both submaximal and maximal insulin-stimulated 2DG transport in incubated isolated soleus and EDL muscle was unaffected by PAK1 KO (Figure 3E-F). This is in contrast to the results using the group I PAK inhibitor IPA-3 (Figure 1) and a previous study in PAK1 KO mice reporting impaired glucose tolerance due to reduced insulin production in pancreatic beta cells together with defects in GLUT4 translocation in skeletal muscle (19).

PAK1 does not regulate in vivo insulin-stimulated glucose uptake nor does PAK1 KO exacerbate high-fat diet-induced insulin resistance. Because our findings in chow fed PAK1 KO mice conflicted with previous reports *in vivo* (19), we further explored the effect of PAK1 KO on glucose uptake in skeletal muscle *in vivo*. Furthermore, we fed a subgroup of the PAK1 KO mice and control littermates a 60E% high-fat diet (HFD 60E%) for 21 weeks. Like for chow fed mice, lack of PAK1 in HFD fed mice had no effect on body composition (Figure 4A-B). Similarly, glucose tolerance (Figure 4C) and plasma insulin concentration during the GTT (Figure 4D) were unaffected by PAK1 KO in HFD fed mice. At the terminal experiment, chow fed mice weighed approximately 26 g, while the HFD group weighted approximately 37 g by the end of the 21 week diet intervention, regardless of genotype (Figure 4E). Energy intake was monitored in a separate experiment and found to be increased (+98%) in mice fed a HFD (Supplemental figure 1A). No effect of genotype was observed (Supplemental figure 1A).

To investigate insulin action, we analyzed insulin-stimulated glucose uptake *in vivo*; a physiological functional outcome of insulin action. Basal blood glucose levels were neither affected by diet nor genotype (Supplemental figure 1B). Insulin administration lowered blood glucose levels by 5.4 mM (-47%) in chow fed control mice, whereas HFD induced a marked insulin resistance with only a 3.0 mM (-26%) drop in blood glucose upon insulin administration (Figure 4F, Supplemental figure 1B).

Lack of PAK1 had no impact on whole body insulin tolerance on neither of the diets (Figure 4F, Supplemental figure 1B). Insulin increased 2DG uptake in chow fed (gastrocnemius: 8.1-fold; quadriceps: 8.5-fold, triceps brachii: 12.3-fold) and HFD fed (gastrocnemius: 3.5-fold; quadriceps: 1.8-fold, triceps brachii: 4.3-fold) control mice (Figure 4G-I). Consistent with our *in vitro* findings, we observed no effect of PAK1 KO on neither basal nor insulin-stimulated 2DG uptake and muscular HFD-induced insulin resistance was induced similarly in both genotypes in all of the investigated muscles (Figure 4G-I). As an estimate of glucose uptake, 2DG uptake accounts for the mass action of the blood glucose concentration in contrast to 2DG clearance. However, 2DG clearance showed similar results as 2DG uptake in all of the investigated muscles (Supplemental figure 1C-E). Thus, PAK1 is not important for *in vivo* insulin-stimulated glucose uptake nor does PAK1 KO exacerbate high-fat diet-induced insulin resistance.

PAK1 is dispensable for contraction-stimulated glucose transport. We next investigated the impact of PAK1 KO on 2DG transport in isolated soleus and EDL muscles in response to electrically-induced contraction. In contrast to IPA-3-treated muscles (Figure 2), we observed no effect of PAK1 KO on contraction-stimulated 2DG transport in neither soleus nor EDL muscle (Figure 5A-B). Moreover, PAK1 KO did not affect initial force development in contracting muscles (Figure 5C). Thus, contrasting with previous findings of abolished *in vivo* insulin-stimulated GLUT4 translocation in these mice (19), our findings show that PAK1 is clearly dispensable for insulin- and contraction-stimulated glucose transport in mouse skeletal muscle.

PAK2 regulates TBC1D4 protein expression and signaling. Because of our discrepant results using the pharmacological inhibitor of group I PAKs and the PAK1 KO mice, we next sought to specifically test the relative contribution and involvement of PAK1 and PAK2 in insulin signaling and glucose transport. For this, we obtained a new cohort of littermate mice that lacked either PAK1 in all tissues of the body (PAK1 KO) or PAK2 specifically in skeletal muscle (PAK2 mKO), or

lacked PAK1 and PAK2 jointly (d1/2KO). While no band for PAK1 could be detected in PAK1 KO muscles, mice lacking PAK2 mice displayed only a 39-59% reduction in band intensity in the immunoblots for PAK2 (Supplemental figure 2A-D, Figure 6K). This is likely due to the fact that the PAK1 KO was whole body knockouts, while the PAK2 mKO was muscle-specific and contaminating tissues could thus contribute to the signal obtained in the PAK2 blots.

Because of similar results in the PAK1 KO mice *in vivo* and *in vitro,* we investigated these mice *in vitro* because it better mimics GLUT4 translocation and in order to use a paired design and analyze basal- and insulin-stimulated signaling and glucose transport in the same mouse to maximize information output. All genotypes displayed normal basal- and insulin-stimulated pAktS473 and pAktT308 in both soleus (Figure 6A+C) and EDL muscle (Figure 6B+D) compared to control littermates. In addition, total Akt2 protein expression was similar in all groups (Supplemental figure 2E-F, Figure 6K) suggesting that neither PAK1 nor PAK2 are regulators of Akt in mouse skeletal muscle. In contrast, protein expression of Akt's downstream target, TBC1D4 was increased by lack of PAK2 in soleus muscle (PAK2 mKO: +47%; d1/2KO: +20%) (Figure 6E), while reduced in EDL (PAK2 mKO: -33%; d1/2KO: -9%) (Figure 6F). However, basal- and insulin-stimulated pTBC1D4 T642 was unaffected in soleus muscle (Figure 6G), suggesting that activation through this pathway is normal. In EDL muscle, insulin-stimulated pTBC1D4 T642 was reduced by lack of PAK2 (PAK2 mKO: -39%; d1/2KO: -4%) (Figure 6H), which could due to the reduced amount of total protein in this muscle. GLUT4 protein was normal in soleus (Figure 6I) and mildly reduced in EDL PAK1 KO and PAK2 mKO mice, but surprisingly not d1/2KO (Figure 6J). Thus, these findings demonstrate that PAK2 regulates TBC1D4 protein expression and signaling in response to insulin in EDL muscle.

Insulin-stimulated glucose transport relies partially on PAK2 in EDL, but not soleus muscle, while PAK1 is not involved. Regardless of genotype, all mice displayed completely normal insulin-

stimulated 2DG transport in isolated soleus muscles compared to control littermates (Figure 7A), suggesting that neither PAK1 nor PAK2 are major regulators of insulin-stimulated glucose transport in soleus muscle. In EDL we observed a modest (PAK2 mKO: -18%; d1/2KO: -12%) reduction of insulin-stimulated 2DG transport in muscles lacking PAK2 (Figure 7B), suggesting that PAK2 may play a minor role in insulin-stimulated glucose transport in glycolytic EDL muscle.

Taken together, our systematic delineation of the involvement of the PAK isoforms expressed in skeletal muscle, consistently show that PAK1 is not involved in glucose uptake in skeletal muscle, while PAK2 may play a minor role.

Discussion

The major finding of the current investigation was that despite previous reports, group I PAKs seem to play no, or modest roles in glucose uptake in skeletal muscle. Using two different cohorts of transgenic mice lacking either PAK1 alone, PAK2, or jointly lacking both PAK1 and PAK2, we show that PAK1 plays no role in neither insulin- nor contraction-stimulated glucose transport in skeletal muscle. On the other hand, PAK2 does seem to be modestly involved in insulin-stimulated glucose transport in EDL muscle, an effect that was accompanied by a reduction in insulin-stimulated pTBC1D4 T642. We also found no effect of whole body KO of PAK1 on glucose tolerance and insulin secretion in mice fed a standard chow diet (insulin sensitive mice) nor in mice fed a HFD (insulin resistant mice). Although glucose uptake has never been assessed before in these mice, our findings are somewhat dissimilar to previous studies showing that in hindblimb muscle of PAK1 KO mice, GLUT4 abundancy at the plasma membrane in response to insulin was completely abrogated (19). That study indicated a key role for PAK1 in regulating glucose transport and therefore we were surprised to find that in all of our experimental models group I PAKs played no,

or only a very modest role in insulin and contraction-stimulated glucose uptake. PAK1 KO mice have also been reported to display impaired glucose tolerance (19,20), whereas in our study PAK1 KO mice on both a chow diet and HFD displayed blood glucose concentrations similar to WT littermates during a glucose tolerance test. The discrepancies are difficult to delineate but could be due to methodological differences. Wang et al. used a crude fractionation method to measure GLUT4 translocation, we analyzed the direct outcome hereof, glucose uptake. Discrepancies between the presence of GLUT4 at the plasma membrane and glucose transport have been reported (34–37). While our studies were conducted in female and male mice at different ranges of ages, but primarily young mice, the past studies on PAK1 KO mice have been conducted in older male mice. Thus the discrepancies could be due to effect of age and a role for PAKs in age- related insulin resistance should be further investigated. Nevertheless, our systemic investigation suggests that group I PAKs are not major players in regulating whole body glucose homeostasis or skeletal muscle glucose uptake.

In the current study, pharmacological inhibition of group I PAKs inhibited muscle glucose transport in response to insulin and contraction. In agreement, IPA-3 inhibited insulin-stimulated GLUT4 translocation and glucose transport in L6 cells (16). However, these effects seemed to be somewhat unspecific as they were not recapitulated in mice lacking PAK1 while only modest effects were found in mice lacking PAK2. IPA-3 is a non-ATP-competitive inhibitor that allosterically inhibit all group 1 PAKs (PAK1, 2, and 3) by binding covalently to the PAK regulatory domain, preventing binding to PAK activators, such as Rac1 (30). Although IPA-3 is described as a highly selective and well described inhibitor of Group 1 PAKs that does not affect other groups of PAK or similar kinases tested (30), off target effects of pharmacological inhibitors is a concern. It also possible, that acute IPA-3-induced inhibition of group I PAKs elicits more potent effects compared with PAK1/2

KO, as the transgenic manipulations have been present from birth and thus could have resulted in compensatory mechanisms. The development of inducible models could help clarify this.

Our hypothesis was that PAKs would be significantly involved in glucose uptake because of the key role of its upstream activator, Rac1 (7,9,23). However, this was not the case, and the question remains as to how Rac1 mediates glucose uptake in muscle. Our findings firmly show that group I PAKs is largely dispensable for normal regulation of glucose transport, suggesting that Rac1 does not mediate glucose uptake through group I PAKs. Another downstream target of Rac1, RalA was recently discovered to act on glucose transport. Overexpression of a constitutively activated Rac1 mutant was found to activate RalA (38) and importantly, expression of a dominant-negative mutant of RalA significantly reduced GLUT4 translocation in response to insulin, and this effect persisted in muscle expressing a constitutively activated mutant of Rac1 (39). Those findings suggest that RalA may mediate the effects on GLUT4 downstream of Rac1. Another recent study has suggested that Rac1 mediate exercise-stimulated glucose uptake through activation of the NADPH oxidase complex and regulated the generation of reactive oxygen species (40). Thus future studies should aim to investigate such players downstream of Rac1, as group I PAKs seems to be largely dispensable for glucose uptake in skeletal muscle.

Based on the present results, we conclude that PAK1/2 proteins are not major regulators of skeletal muscle glucose uptake but that PAK2 may play a minor role.

Disclosure summary: No potential conflicts of interest relevant to this article were reported.

Grants: This study was supported by a PhD fellowship from The Lundbeck Foundation (grant 2015-3388 to LLVM); The Danish Council for Independent Research, Medical Sciences (grant DFF-4004-00233 to LS, grant 6108-00203 to EAR); The Novo Nordisk Foundation (grant 10429 to EAR, grant NNF16OC0023418 and NNF18OC0032082 to LS).

Acknowledgements:

We thank our colleagues at the Section of Molecular Physiology, Department of Nutrition, Exercise, and Sports (NEXS), Faculty of Science, University of Copenhagen (UC), for fruitful discussions on this topic. We acknowledge the skilled technical assistance of Betina Bolmgren, Irene B. Nielsen, Mona Ali and Nicoline R. Andersen (Section of Molecular Physiology, NEXS, Faculty of Science, UC, Denmark). The PAK1 KO mice were a kind gift from Debbie Thurmond (Department of Molecular & Cellular Endocrinology, Diabetes and Metabolism Research Institute, City of Hope/BRICA, USA).

1. DeFronzo RA, Gunnarsson R, Bjorkman O, Olsson M, Wahren J. Effects of insulin on peripheral and splanchnic glucose metabolism in noninsulin-dependent (type II) diabetes mellitus. J Clin Invest. 1985;76(1):149–55.
2. Samuel VT, Petersen KF, Shulman GI. Lipid-induced insulin resistance: unravelling the mechanism. Lancet (London, England). 2010 Jun;375(9733):2267–77.
3. Lauritzen HPMM. Insulin- and contraction-induced glucose transporter 4 traffic in muscle: insights from a novel imaging approach. Exerc Sport Sci Rev. 2013 Apr;41(2):77–86.
4. Sano H, Kane S, Sano E, Miinea CP, Asara JM, Lane WS, et al. Insulin-stimulated phosphorylation of a Rab GTPase-activating protein regulates GLUT4 translocation. J Biol Chem. 2003 Apr;278(17):14599–602.
5. Kramer HF, Witczak CA, Taylor EB, Fujii N, Hirshman MF, Goodyear LJ. AS160 regulates insulin- and contraction-stimulated glucose uptake in mouse skeletal muscle. J Biol Chem. 2006;281(42):31478–85.
6. Ueda S, Kataoka T, Satoh T. Activation of the small GTPase Rac1 by a specific guanine-nucleotide-exchange factor suffices to induce glucose uptake into skeletal-muscle cells. Biol cell. 2008 Nov;100(11):645–57.

7. JeBailey L, Wanono O, Niu W, Roessler J, Rudich A, Klip A. Ceramide- and oxidant-induced insulin resistance involve loss of insulin-dependent Rac-activation and actin remodeling in muscle cells. Diabetes. 2007 Feb;56(2):394–403.

8. Ueda S, Kitazawa S, Ishida K, Nishikawa Y, Matsui M, Matsumoto H, et al. Crucial role of the small GTPase Rac1 in insulin-stimulated translocation of glucose transporter 4 to the mouse skeletal muscle sarcolemma. FASEB J Off Publ Fed Am Soc Exp Biol. 2010 Jul;24(7):2254–61.

9. Sylow L, Jensen TE, Kleinert M, Hojlund K, Kiens B, Wojtaszewski J, et al. Rac1 Signaling Is Required for Insulin-Stimulated Glucose Uptake and Is Dysregulated in Insulin-Resistant Murine and Human Skeletal Muscle. Diabetes. 2013 Jun;62(6):1865–75.

10. Sylow L, Møller LLV, Kleinert M, D'Hulst G, De Groote E, Schjerling P, et al. Rac1 and AMPK Account for the Majority of Muscle Glucose Uptake Stimulated by Ex Vivo Contraction but Not In Vivo Exercise. Diabetes. 2017 Jun;66(6):1548–59.

11. Sylow L, Jensen TE, Kleinert M, Mouatt JR, Maarbjerg SJ, Jeppesen J, et al. Rac1 is a novel regulator of contraction-stimulated glucose uptake in skeletal muscle. Diabetes. 2013;62(4).

12. Sylow L, Møller LL V., Kleinert M, Richter EA, Jensen TE. Stretch-stimulated glucose transport in skeletal muscle is regulated by Rac1. J Physiol. 2015 Feb;593(3):645–56.

13. Manser E, Chong C, Zhao ZS, Leung T, Michael G, Hall C, et al. Molecular cloning of a new member of the p21-Cdc42/Rac-activated kinase (PAK) family. J Biol Chem. 1995 Oct;270(42):25070–8.

14. Joseph GA, Lu M, Radu M, Lee JK, Burden SJ, Chernoff J, et al. Group I Paks Promote Skeletal Myoblast Differentiation In Vivo and In Vitro. Mol Cell Biol. 2017 Feb;37(4).

15. Chiang YA, Jin T. p21-Activated protein kinases and their emerging roles in glucose homeostasis. Am J Physiol Endocrinol Metab. 2014 Apr;306(7):E707-22.

16. Tunduguru R, Chiu TT, Ramalingam L, Elmendorf JS, Klip A, Thurmond DC. Signaling of the p21-activated kinase (PAK1) coordinates insulin-stimulated actin remodeling and glucose uptake in skeletal muscle cells. Biochem Pharmacol. 2014 Nov;92(2):380–8.

17. Tsakiridis T, Taha C, Grinsteinl S, Klip A. Insulin activates a p21-activated kinase in muscle cells via phosphatidylinositol 3-kinase. J Biol Chem. 1996 Aug;271(33):19664–7.

18. Stierwalt HD, Ehrlicher SE, Bergman BC, Robinson MM, Newsom SA. Insulin-stimulated Rac1-GTP binding is not impaired by palmitate treatment in L6 myotubes. Physiol Rep. 2018 Dec;6(24):e13956.

19. Wang Z, Oh E, Clapp DW, Chernoff J, Thurmond DC. Inhibition or ablation of p21-activated kinase (PAK1) disrupts glucose homeostatic mechanisms in vivo. J Biol Chem. 2011 Dec;286(48):41359–67.

20. Ahn M, Yoder SM, Wang Z, Oh E, Ramalingam L, Tunduguru R, et al. The p21-activated kinase (PAK1) is involved in diet-induced beta cell mass expansion and survival in mice and human islets. Diabetologia. 2016 Oct;59(10):2145–55.

21. Allen JD, Jaffer ZM, Park SJ, Burgin S, Hofmann C, Sells MA, et al. P21-activated kinase regulates mast cell degranulation via effects on calcium mobilization and cytoskeletal dynamics. Blood. 2009;113(12):2695–705.

22. Viollet B, Andreelli F, Jørgensen SB, Perrin C, Geloen A, Flamez D, et al. The AMP-activated protein kinase α2 catalytic subunit controls whole-body insulin sensitivity. J Clin Invest. 2003 Jan;111(1):91–8.

23. Raun SH, Ali M, Kjøbsted R, Møller LL V., Federspiel MA, Richter EA, et al. Rac1 muscle knockout exacerbates the detrimental effect of high-fat diet on insulin-stimulated muscle glucose uptake

independently of Akt. J Physiol. 2018 Jun;596(12):2283–99.

24. Strömblad G, Björntorp P. Reduced hepatic insulin clearance in rats with dietary-induced obesity. Metabolism. 1986;35(4):323–7.

25. Brandimarti P, Costa-Júnior JM, Ferreira SM, Protzek AO, Santos GJ, Carneiro EM, et al. Cafeteria diet inhibits insulin clearance by reduced insulindegrading enzyme expression and mRNA splicing. J Endocrinol. 2013;219(2):173–82.

26. Jung S-H, Jung C-H, Reaven GM, Kim SH. Adapting to insulin resistance in obesity: role of insulin secretion and clearance. Diabetologia. 2018;61(3):681–7.

27. Ferre P, Leturque A, Burnol A-F, Penicaud L, Girard J. A method to quantify glucose utilization in vivo in skeletal muscle and white adipose tissue of the anaesthetized rat. Biochem J. 1985;228(1):103–10.

28. Fueger PT, Bracy DP, Malabanan CM, Pencek RR, Wasserman DH. Distributed control of glucose uptake by working muscles of conscious mice: roles of transport and phosphorylation. Am J Physiol Metab. 2004;286(1):E77–84.

29. Welinder C, Ekblad L. Coomassie staining as loading control in Western blot analysis. J Proteome Res. 2011;10(3):1416–9.

30. Deacon SW, Beeser A, Fukui JA, Rennefahrt UEE, Myers C, Chernoff J, et al. Article An Isoform-Selective, Small-Molecule Inhibitor Targets the Autoregulatory Mechanism of p21-Activated Kinase.

31. Molero JC, Jensen TE, Withers PC, Couzens M, Herzog H, Thien CBF, et al. c-Cbl-deficient mice have reduced adiposity, higher energy expenditure, and improved peripheral insulin action. J Clin Invest. 2004 Nov;114(9):1326–33.

32. Kjøbsted R, Munk-Hansen N, Birk JB, Foretz M, Viollet B, Björnholm M, et al. Enhanced muscle insulin sensitivity after contraction/exercise is mediated by AMPK. Diabetes. 2017;66(3).

33. O'Neill HM, Maarbjerg SJ, Crane JD, Jeppesen J, Jorgensen SB, Schertzer JD, et al. AMP-activated protein kinase (AMPK) beta1beta2 muscle null mice reveal an essential role for AMPK in maintaining mitochondrial content and glucose uptake during exercise. Proc Natl Acad Sci U S A. 2011 Sep;108(38):16092–7.

34. Ng Y, Ramm G, Lopez JA, James DE. Rapid activation of Akt2 is sufficient to stimulate GLUT4 translocation in 3T3-L1 adipocytes. Cell Metab. 2008 Apr;7(4):348–56.

35. Somwar R, Kim DY, Sweeney G, Huang C, Niu W, Lador C, et al. GLUT4 translocation precedes the stimulation of glucose uptake by insulin in muscle cells: potential activation of GLUT4 via p38 mitogen-activated protein kinase. Biochem J. 2001 Nov;359(Pt 3):639–49.

36. Somwar R, Niu W, Kim DY, Sweeney G, Randhawa VK, Huang C, et al. Differential effects of phosphatidylinositol 3-kinase inhibition on intracellular signals regulating GLUT4 translocation and glucose transport. J Biol Chem. 2001 Dec;276(49):46079–87.

37. Funaki M, Benincasa K, Randhawa PK. Peptide rescues GLUT4 recruitment, but not GLUT4 activation, in insulin resistance. Biochem Biophys Res Commun. 2007 Sep;360(4):891–6.

38. Nozaki S, Ueda S, Takenaka N, Kataoka T, Satoh T. Role of RalA downstream of Rac1 in insulin-dependent glucose uptake in muscle cells. Cell Signal. 2012 Nov;24(11):2111–7.

39. Takenaka N, Sumi Y, Matsuda K, Fujita J, Hosooka T, Noguchi T, et al. Role for RalA downstream of Rac1 in skeletal muscle insulin signalling. Biochem J. 2015 Aug;469(3):445–54.

40. Henriquez-Olguin, C., Knudsen, J.R., Raun, S.H., Li, Z., Dalbram, E., Treebak, J.T., Sylow, L., Holmdahl, R., Richter, E.A., Jaimovich, E., and Jensen T. Title Exercise-stimulated muscle ROS production and glucose uptake requires NADPH oxidase 2. 2019;

Figure Legends

Figure 1: Insulin-stimulated glucose transport is reduced in IPA-3-treated mouse soleus muscle. A-B) Insulin-stimulated (60 nM) 2 Deoxy-glucose (2DG) transport in soleus (A) and extensor digitorum longus (EDL, B) muscle ± 40 µM IPA-3 or a corresponding amount of DMSO. Pre-incubation for 25 minutes followed by 30 minutes insulin stimulation with 2DG transport analyzed for the final 10 minutes of stimulation. **C-H)** Bar graphs showing quantification of phosphorylated (p)PAK1 T423, pAkt S473, and pAkt T308 in insulin-stimulated soleus (C, E, and G) and EDL (D, F, and H) muscle ± 40 µM IPA-3 or a corresponding amount of DMSO. Samples were excluded in some of the immunoblots, so the number of determinations were *n = 8/8* (DMSO/IPA-3) for pPAK1 T423 and *n = 8/7* for pAkt S473 and T308 in soleus muscle were. **I-J)** Representative blots showing pPAK1 T423, pAkt S473, and pAkt T308 in soleus (I) and EDL (J) muscle. Interactions: Insulin stimulation vs. basal control *** ($p<0.001$); IPA-3 vs. DMSO control #/### ($p<0.05/0.001$). Unless otherwise stated in the figure legend, the number of determinations in each group: DMSO, *n = 9/9* (soleus/EDL); IPA-3, *n = 8/8*. Data are presented as mean ± S.E.M. with individual values shown. A.U., arbitrary units.

Figure 2: Contraction-stimulated glucose transport is partially inhibited in IPA-3-treated mouse skeletal muscle. A-B) Contraction-stimulated (2 sec/15 sec, 100 Hz) 2 Deoxy-glucose (2DG) transport in soleus (A) and extensor digitorum longus (EDL, B) muscle ± 40 µM IPA-3 or a corresponding amount of DMSO. Pre-incubation for 45 minutes followed by 15 minutes electrically-stimulated contractions with 2DG transport analyzed for the final 10 minutes of stimulation. **C)** Initial force development during electrically-stimulated contractions in soleus and EDL muscle ± 40 µM IPA-3 or a corresponding amount of DMSO. **D-G)** Bar graphs showing quantification of phosphorylated (p)AMPK T172 and pACC2 S212 in contraction-stimulated soleus (D and F) and EDL (E and G) muscle ± 40 µM IPA-3 or a corresponding amount of DMSO.

Samples were excluded in the immunoblot for pACC2 S212 in soleus muscle and the number of determinations were *n = 5/6* (DMSO/IPA-3). **H-I)** Representative blots showing pAMPK T172 and pACC2 S212 and actin protein expression as a loading control in soleus (H) and EDL (I) muscle. Interactions: Insulin stimulation vs. basal control **/*** ($p<0.01/0.001$); IPA-3 vs. DMSO control #/## ($p<0.05/0.01$). Unless otherwise stated in the figure legend, the number of determinations in each group: DMSO, *n = 8/8* (soleus/EDL); IPA-3, *n = 9/9*. Data are presented as mean ± S.E.M. with individual values shown. A.U., arbitrary units.

Figure 3: PAK1 knockout does not affect whole body glucose homeostasis or insulin-stimulated glucose transport in isolated skeletal muscle. A-B) Bar graph showing body composition (FM: Fat mass; LBM: Lean body mass; BM: Body mass) in gram (A) or percentage (B) in chow fed PAK1 knockout (KO) mice or control littermates. Mice were 7-19 weeks of age. The number of mice in each group: Control, *n = 13*; PAK1 KO, *n = 12*. **C)** Blood glucose levels during a glucose tolerance test (GTT) in chow fed PAK1 KO mice or control littermates. Mice were 8-20 weeks of age. The number of mice in each group: Control, *n = 10*; PAK1 KO, *n = 9*. **D)** Plasma insulin values during GTT in chow fed PAK1 KO mice or control littermates. Mice were 9-21 weeks of age. The number of mice in each group: Control, *n = 13*; PAK1 KO, *n = 10*. **E-F)** Submaximal (6 nM) and maximal (60 nM) insulin-stimulated 2 Deoxy-glucose (2DG) transport in soleus (A) and extensor digitorum longus (EDL, B) muscle from PAK1 KO mice or littermate controls. Mice were 12-24 weeks of age. Pre-incubation for 30 minutes followed by 30 minutes insulin stimulation with 2DG transport analyzed for the final 10 minutes of stimulation. The number of determinations in each group: Control-Basal, *n = 13/12* (soleus/EDL); Control-Submaximal, *n = 6/6*; Control-Maximal, *n = 7/6*; PAK1 KO-Basal, *n = 14/14*; Control-Submaximal, *n = 7/7*; Control-Maximal, *n = 7/7*. ¤¤¤ Main effect of maximal vs. submaximal insulin stimulation ($p<0.001$). Data are presented as mean ± S.E.M. or mean ± S.E.M. with individual values shown.

Figure 4: PAK1 does not regulate *in vivo* insulin-stimulated glucose uptake in mouse skeletal muscle. A-B) Bar graph showing body composition (FM: Fat mass; LBM: Lean body mass) in gram (A) or percentage (B) in PAK1 knockout (KO) mice or control littermates fed a 60E% high-fat diet (HFD 60E%) for 21 weeks. Body composition was measured in week 18-19. The number of mice in each group: Control, *n = 14*; PAK1 KO, *n = 17*. **C)** Blood glucose levels during a glucose tolerance test (GTT) in PAK1 KO mice or control littermates fed a HFD 60E% for 21 weeks. Glucose tolerance was measured in week 14. The number of mice in each group: Control, *n = 13*; PAK1 KO, *n = 17*. **D)** Plasma insulin values during GTT in HFD 60E% fed PAK1 KO mice or control littermates fed a HFD 60E% for 21 weeks. Plasma insulin in response to glucose administration was measured in week 16. The number of mice in each group: Control, *n = 11*; PAK1 KO, *n = 16*. **E)** Body mass at terminal experiment in PAK1 KO mice or control littermates. Chow fed mice fed were terminated at 10-24 weeks of age. Mice fed a HFD 60E% for 21 weeks were terminated at 27-37 weeks of age. The number of mice in each group: Control, *n = 22/14* (Chow/HFD 60E%); PAK1 KO, *n = 10/16*. **F)** Blood glucose levels related to basal during retro orbital insulin tolerance test (ITT) in PAK1 KO mice or control littermates fed a HFD 60E% or chow diet. The number of mice in each group: Control, *n = 12/10* (Chow/HFD 60E%); PAK1 KO, *n = 6/11*. **G-I)** Insulin-stimulated (Chow: 0.5 U kg^{-1} body weight; HFD 60E%: 60% of insulin administered to chow fed mice) 2 Deoxy-glucose (2DG) uptake in gastrocnemius (G), quadriceps (H), and triceps brachii (I) muscle from PAK1 KO mice or control littermates fed a HFD 60E% or chow diet. The number of mice in each group: Control-Saline, *n = 12/6* (Chow/HFD 60E%); Control-Insulin, *n = 12/10* (Chow/HFD 60E%); PAK1 KO-Saline, *n = 4/6*; PAK1 KO-Insulin, *n = 6/11*. *** Main effect of insulin stimulation ($p<0.05/0.001$). §§/§§§ Main effect of HFD 60E% ($p<0.01/0.001$). Data are presented as mean ± S.E.M. or mean ± S.E.M. with individual values shown.

Figure 5: Contraction-stimulated glucose transport is not affected in isolated skeletal muscle from PAK1 knockout mice. A-B) Contraction-stimulated (2 sec/15 sec, 100 Hz) 2 Deoxy-glucose (2DG) transport in soleus (A) and extensor digitorum longus (EDL, B) muscle from PAK1 knockout (KO) mice or littermate controls. Pre-incubation for 30 minutes followed by 15 minutes electrically-stimulated contractions with 2DG transport analyzed for the final 10 minutes of stimulation. **C)** Initial force development during electrically-stimulated contractions in soleus and EDL muscle from PAK1 KO mice or littermate controls. **D-E)** Representative blots showing total PAK1 protein expression in soleus (D) and EDL (E) muscle from PAK1 KO mice or littermate controls. The number of determinations in each group: Control, *n = 9/9* (soleus/EDL); PAK1 KO, *n = 8/9*. Data are presented as mean ± S.E.M. with individual values shown.

Figure 6: Lack of PAK2 affects TBC1D4 protein expression and signaling. A-J) Bar graphs showing quantification of phosphorylation of (p)Akt S473, pAkt T308, pTBC1D4 T642 and total TBC1D4 and GLUT4 protein expression in insulin-stimulated (60 nM) soleus (A, C, E, G, and I) and extensor digitorum longus (B, D, F, H, and J) muscle from PAK1 knockout (KO), PAK2 mKO, PAK1/2 double KO (d1/2KO) mice or littermate controls. Total protein expression is an average of paired basal- and insulin-stimulated sample. The number of determinations for GLUT4 in soleus muscle: Control, *n = 6*; PAK1 KO, *n = 5*; PAK2 KO, *n = 6*; PAK1/2 dKO, *n = 6*. **K-L)** Representative blots showing pAkt S473, pAkt T308, pTBC1D4 T642 and total PAK1, PAK2, Akt2, TBC1D4 and GLUT4 protein expression and coomassie staining as a loading control in soleus (K) and EDL (L) muscle. Total protein expression is an average of paired basal and insulin-stimulated samples. Interactions: Control vs. PAK1 KO § ($p<0.05$); Control vs. PAK2 mKO €€ ($p<0.01$). Unless otherwise stated in the figure legend, the number of determinations in each group: Control, *n = 9/10* (soleus/EDL); PAK1 KO, *n = 8/9*; PAK2 KO, *n = 10/9*; PAK1/2 dKO, *n = 9/9*. Data are presented as mean ± S.E.M. with individual values shown. A.U., arbitrary units.

Figure 7: PAK2 mKO, but not PAK1 KO partly reduces glucose transport in EDL muscle. A-B) Insulin-stimulated (60 nM) 2 Deoxy-glucose (2DG) transport in soleus (A) and extensor digitorum longus (EDL, B) muscle from PAK1 knockout (KO), PAK2 mKO, PAK1/2 double KO (d1/2KO) mice or control littermates. Pre-incubation for 20 minutes followed by 20 minutes insulin stimulation with 2DG transport analyzed for the final 10 minutes of stimulation. The number of determinations in each group: Control, *n = 9/10* (soleus/EDL); PAK1 KO, *n = 8/9*; PAK2 KO, *n = 10/10*; PAK1/2 dKO, *n = 9/9*. Data are presented as mean ± S.E.M. with individual values shown.

Supplemental figure 1: A) Energy intake in chow or 60E% high-fat diet (HFD 60E%) fed PAK1 knockout (KO) mice or control littermates. The number of mice in each group: Control, *n = 8/8* (Chow/HFD 60E%); PAK1 KO, *n = 8/8*. **B)** Blood glucose levels during retro orbital insulin tolerance test (ITT) in chow or HFD 60E% fed PAK1 KO mice or control littermates. The number of mice in each group: Control, *n = 12/10* (Chow/HFD 60E%); PAK1 KO, *n = 6/11*. **C-E)** Insulin-stimulated (Chow: 0.5 U kg^{-1} body weight; HFD 60E%: 60% of insulin administered to chow fed mice) 2 Deoxy-glucose (2DG) clearance in gastrocnemius (C), quadriceps (D), and triceps brachii (E) muscle from PAK1 KO mice or control littermates fed a chow or HFD 60E% diet. The number of mice in each group: Control-Saline, *n = 12/6* (Chow/HFD 60E%); Control-Insulin, *n = 12/10* (Chow/HFD 60E%); PAK1 KO-Saline, *n = 4/6*; PAK1 KO-Insulin, *n = 6/11*. *** Main effect of insulin stimulation ($p<0.05/0.001$). §§§ Main effect of HFD 60E% ($p<0.001$). Data are presented as mean ± S.E.M. or mean ± S.E.M. with individual values shown.

Supplemental figure 2: A-F) Bar graphs showing quantification of total PAK1, PAK2, and Akt2 protein expression in soleus (A, C, and E) and extensor digitorum longus (B, D, and F) muscle from PAK1 knockout (KO), PAK2 mKO, PAK1/2 double KO (d1/2KO) mice or littermate controls.

Total protein expression is an average of paired basal- and insulin-stimulated sample. ¤¤¤ Main effect of PAK1 KO ($p<0.001$). ##/### Main effect of PAK2 KO ($p<0.01/0.001$). The number of determinations in each group: Control, *n = 9/10* (soleus/EDL); PAK1 KO, *n = 8/9*; PAK2 KO, *n = 10/9*; PAK1/2 dKO, *n = 9/9*. Data are presented as mean ± S.E.M with individual values shown. A.U., arbitrary units.

Figure 1

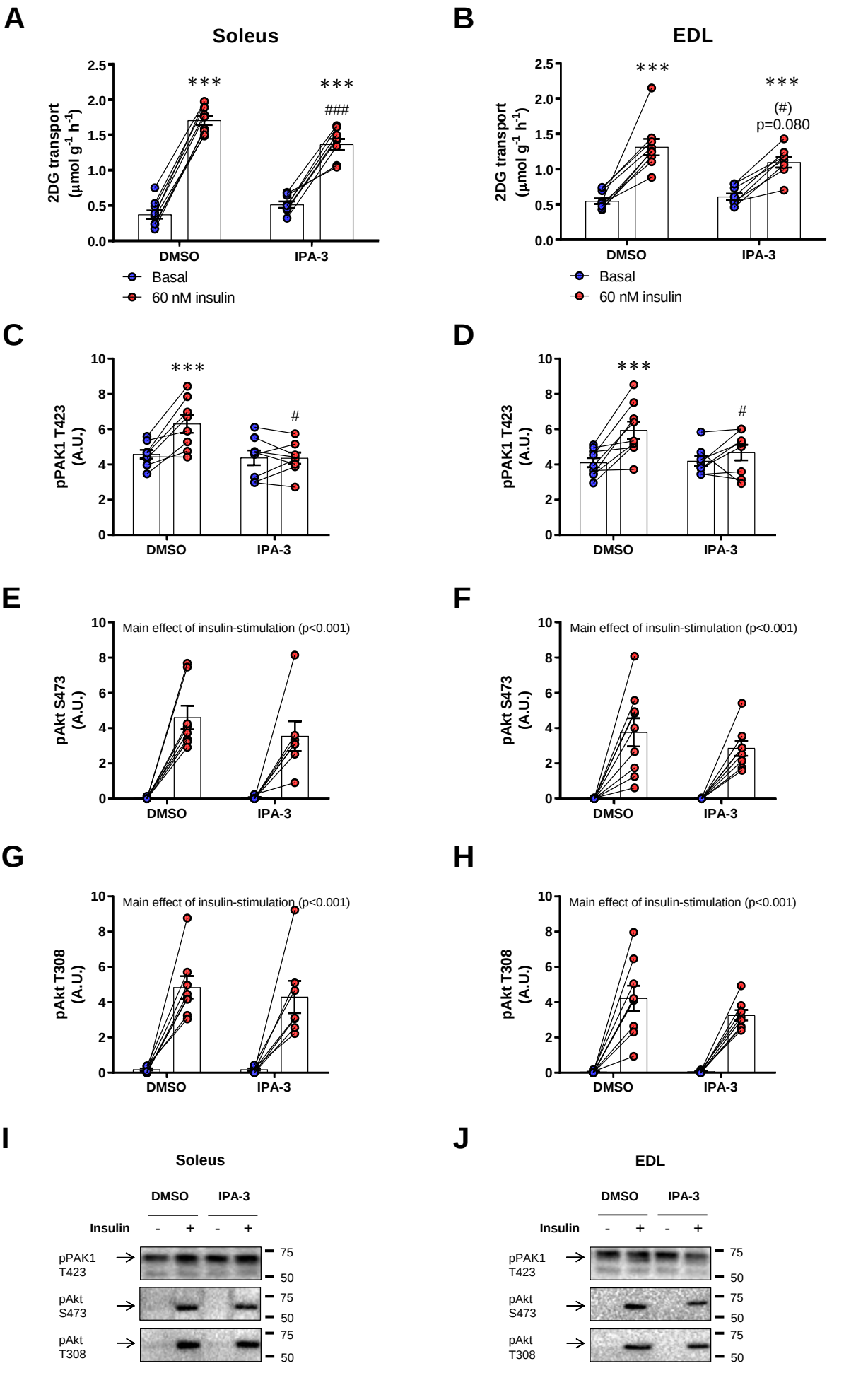
A
Soleus
2DG transport (µmol g-1 h-1)
***
***
###
DMSO
IPA-3
Basal
60 nM insulin
B
EDL
***
***
(#)
p=0.080
C
pPAK1 T423 (A.U.)
***
#
D
***
#
E
pAkt S473 (A.U.)
Main effect of insulin-stimulation (p<0.001)
F
Main effect of insulin-stimulation (p<0.001)
G
pAkt T308 (A.U.)
Main effect of insulin-stimulation (p<0.001)
H
Main effect of insulin-stimulation (p<0.001)
I
Soleus
DMSO
IPA-3
Insulin
- + - +
pPAK1 T423
pAkt S473
pAkt T308
75
50
J
EDL

Figure 2

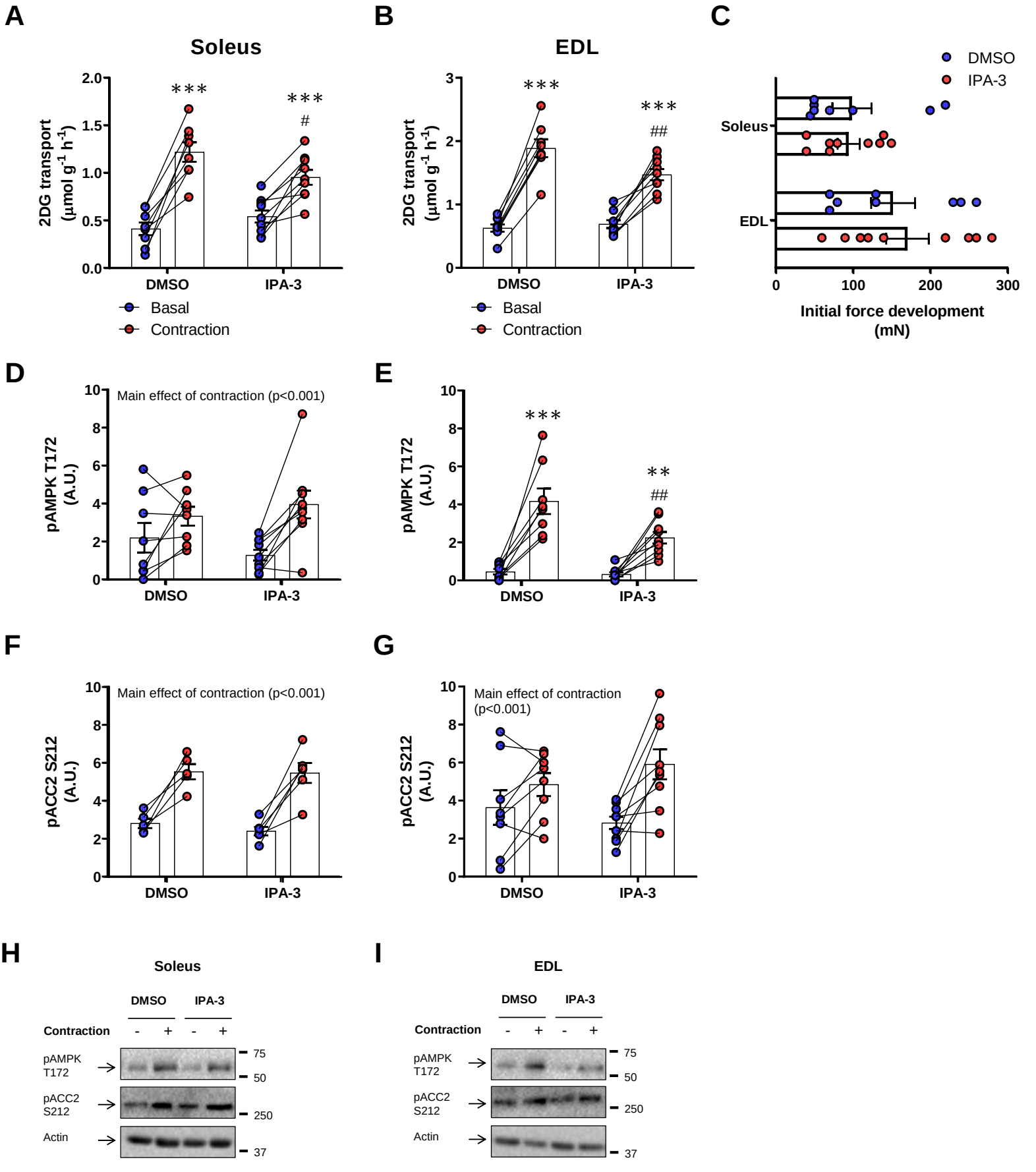
A
Soleus
2DG transport (µmol g-1 h-1)
***
***
#
DMSO
IPA-3
Basal
Contraction
B
EDL
2DG transport (µmol g-1 h-1)
***
***
##
DMSO
IPA-3
Basal
Contraction
C
DMSO
IPA-3
Soleus
EDL
Initial force development (mN)
D
Main effect of contraction (p<0.001)
pAMPK T172 (A.U.)
DMSO
IPA-3
E
***
**
##
pAMPK T172 (A.U.)
DMSO
IPA-3
F
Main effect of contraction (p<0.001)
pACC2 S212 (A.U.)
DMSO
IPA-3
G
Main effect of contraction (p<0.001)
pACC2 S212 (A.U.)
DMSO
IPA-3
H
Soleus
DMSO
IPA-3
Contraction
pAMPK T172
pACC2 S212
Actin
75
50
250
37
I
EDL
DMSO
IPA-3
Contraction
pAMPK T172
pACC2 S212
Actin
75
50
250
37

Figure 3

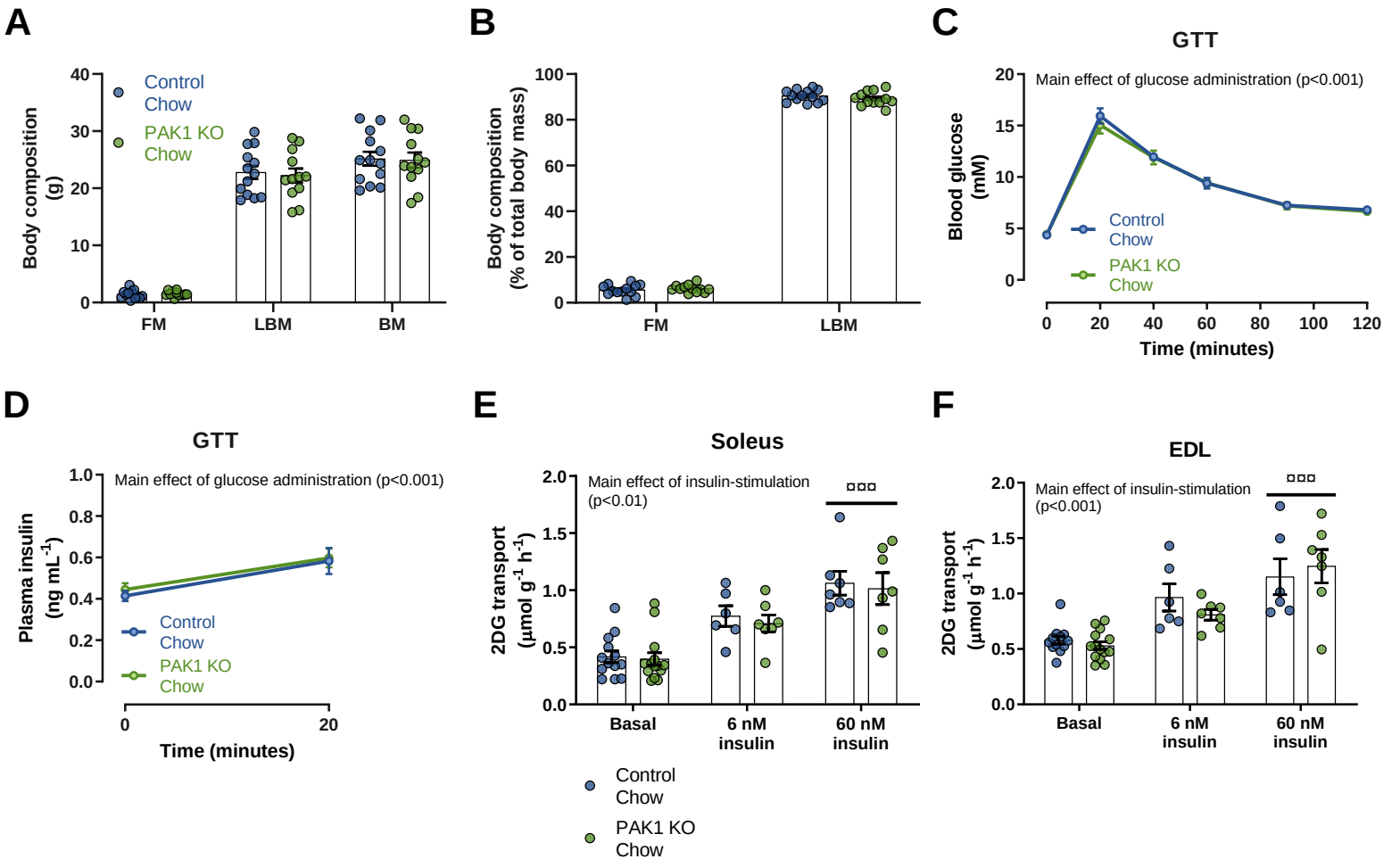
A
Body composition (g)
Control Chow
PAK1 KO Chow
FM
LBM
BM
B
Body composition (% of total body mass)
FM
LBM
C
GTT
Main effect of glucose administration (p<0.001)
Blood glucose (mM)
Control Chow
PAK1 KO Chow
Time (minutes)
D
GTT
Main effect of glucose administration (p<0.001)
Plasma insulin (ng mL-1)
Control Chow
PAK1 KO Chow
Time (minutes)
E
Soleus
Main effect of insulin-stimulation (p<0.01)
¤¤¤
2DG transport (µmol g-1 h-1)
Basal
6 nM insulin
60 nM insulin
Control Chow
PAK1 KO Chow
F
EDL
Main effect of insulin-stimulation (p<0.001)
¤¤¤
2DG transport (µmol g-1 h-1)
Basal
6 nM insulin
60 nM insulin

Figure 4

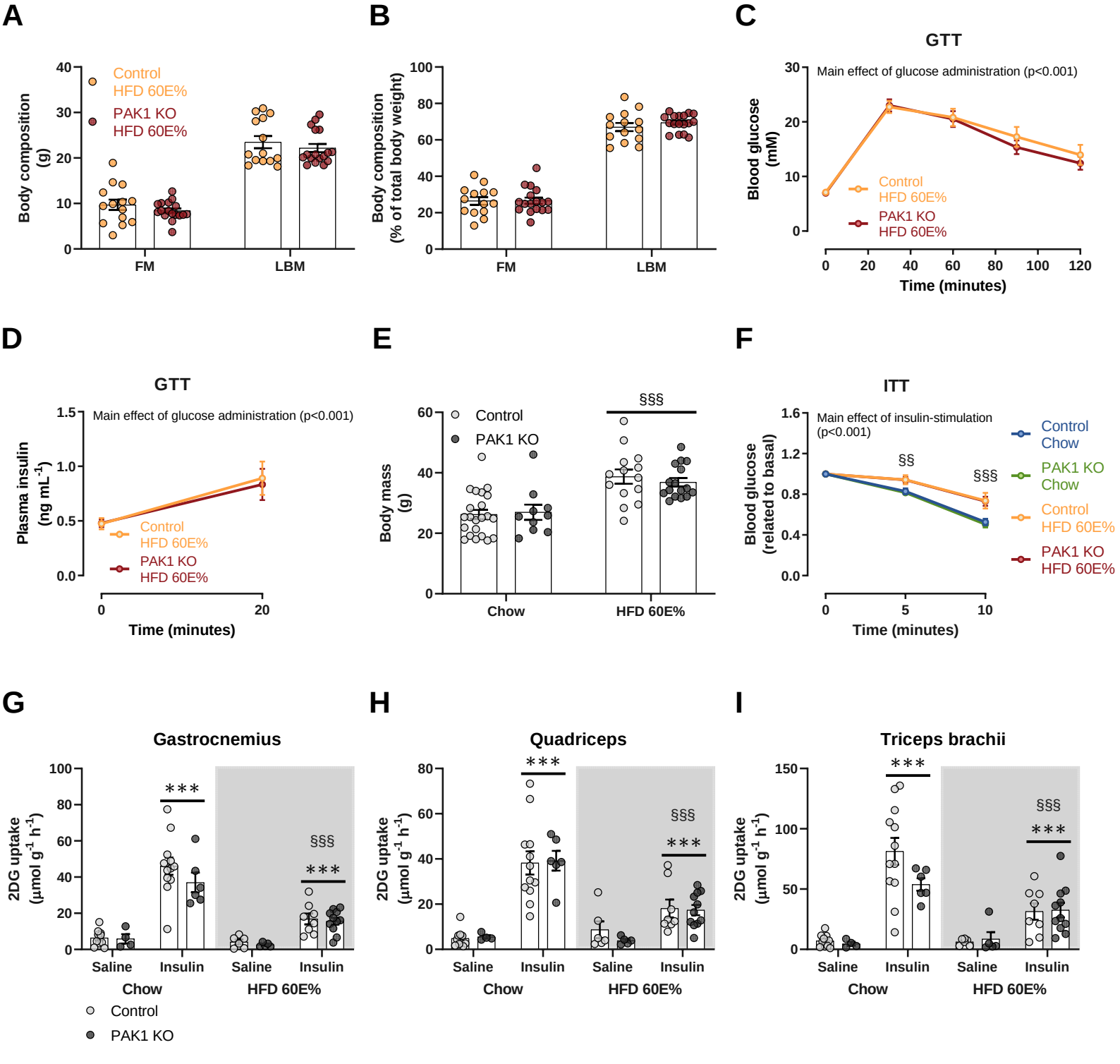
A
Body composition (g)
Control HFD 60E%
PAK1 KO HFD 60E%
FM
LBM
B
Body composition (% of total body weight)
FM
LBM
C
GTT
Main effect of glucose administration (p<0.001)
Blood glucose (mM)
Control HFD 60E%
PAK1 KO HFD 60E%
Time (minutes)
D
GTT
Main effect of glucose administration (p<0.001)
Plasma insulin (ng mL-1)
Control HFD 60E%
PAK1 KO HFD 60E%
Time (minutes)
E
Body mass (g)
Control
PAK1 KO
§§§
Chow
HFD 60E%
F
ITT
Main effect of insulin-stimulation (p<0.001)
Blood glucose (related to basal)
§§
§§§
Control Chow
PAK1 KO Chow
Control HFD 60E%
PAK1 KO HFD 60E%
Time (minutes)
G
Gastrocnemius
2DG uptake (µmol g-1 h-1)
***
§§§
***
Saline
Insulin
Saline
Insulin
Chow
HFD 60E%
Control
PAK1 KO
H
Quadriceps
2DG uptake (µmol g-1 h-1)
***
§§§
***
Saline
Insulin
Saline
Insulin
Chow
HFD 60E%
I
Triceps brachii
2DG uptake (µmol g-1 h-1)
***
§§§
***
Saline
Insulin
Saline
Insulin
Chow
HFD 60E%

Figure 5

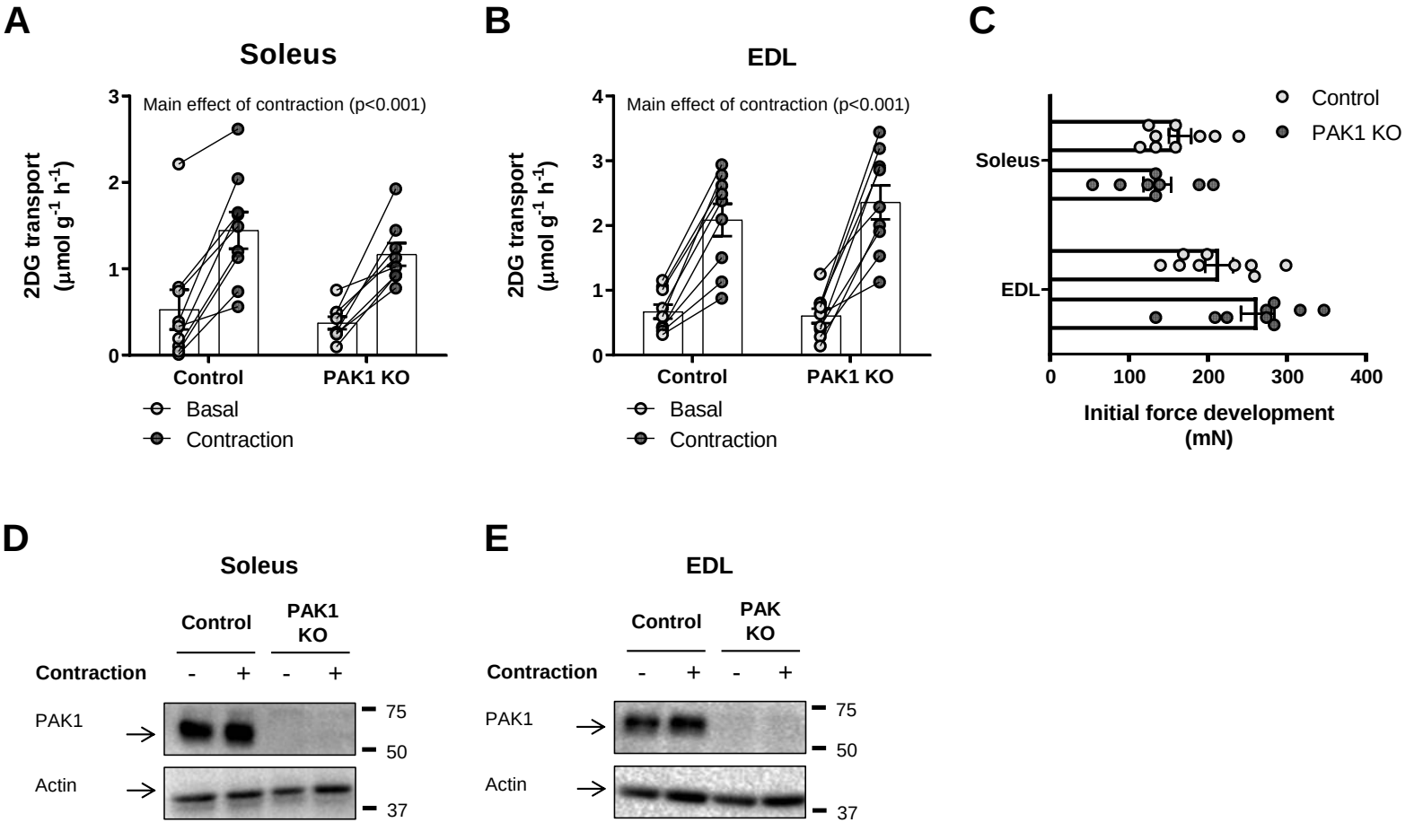
A
Soleus
Main effect of contraction (p<0.001)
2DG transport (µmol g-1 h-1)
Control
PAK1 KO
Basal
Contraction
B
EDL
Main effect of contraction (p<0.001)
2DG transport (µmol g-1 h-1)
Control
PAK1 KO
Basal
Contraction
C
Control
PAK1 KO
Soleus
EDL
Initial force development (mN)
D
Soleus
Control
PAK1 KO
Contraction
PAK1
Actin
75
50
37
E
EDL
Control
PAK KO
Contraction
PAK1
Actin
75
50
37

Figure 6

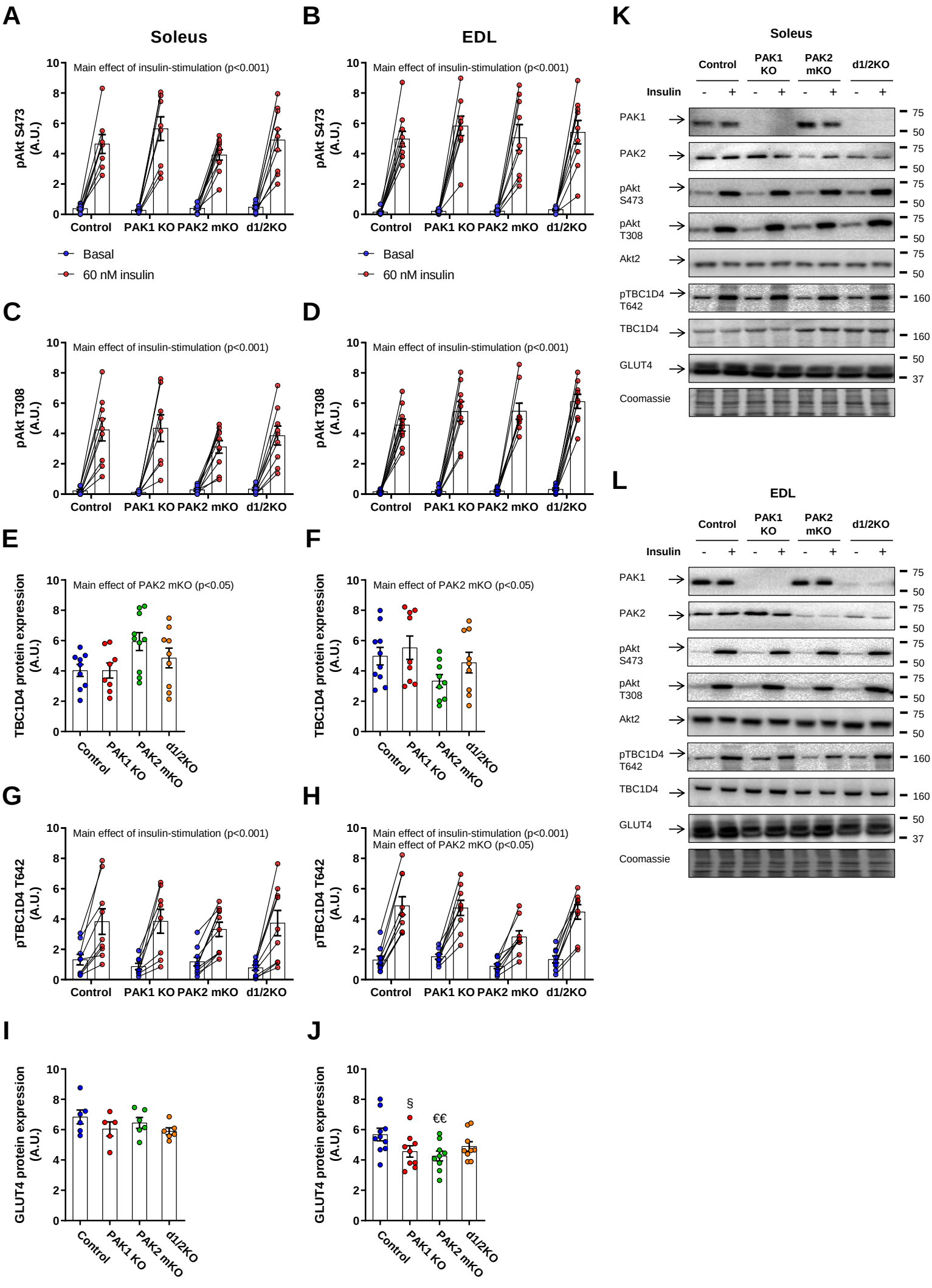

Figure 7

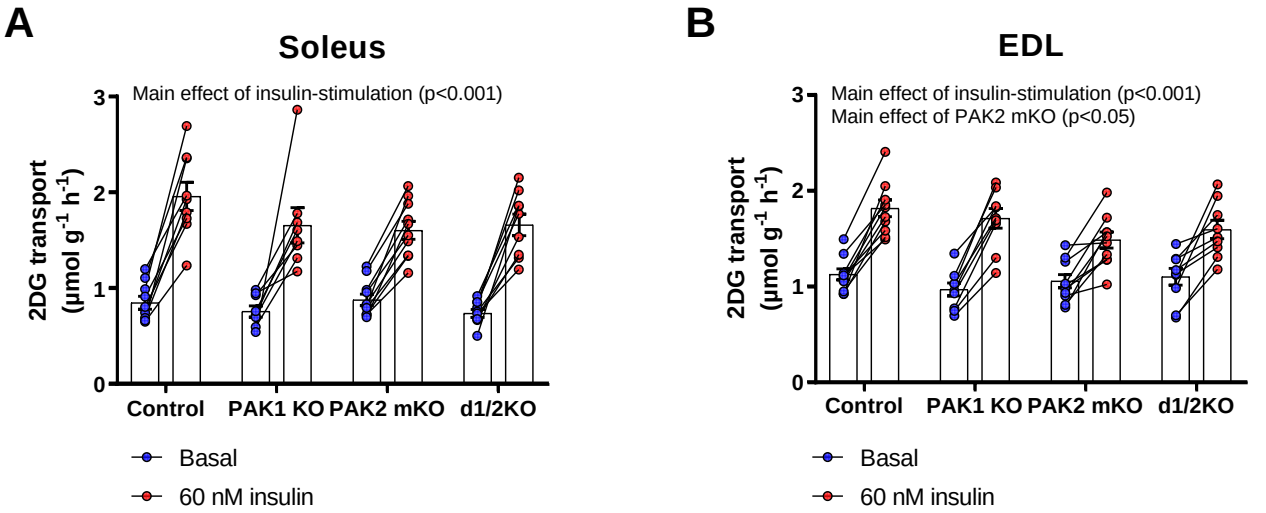
A
Soleus
Main effect of insulin-stimulation (p<0.001)
2DG transport
(µmol g-1 h-1)
3
2
1
0
Control
PAK1 KO
PAK2 mKO
d1/2KO
Basal
60 nM insulin
B
EDL
Main effect of insulin-stimulation (p<0.001)
Main effect of PAK2 mKO (p<0.05)
2DG transport
(µmol g-1 h-1)
3
2
1
0
Control
PAK1 KO
PAK2 mKO
d1/2KO
Basal
60 nM insulin

Supplemental figure 1

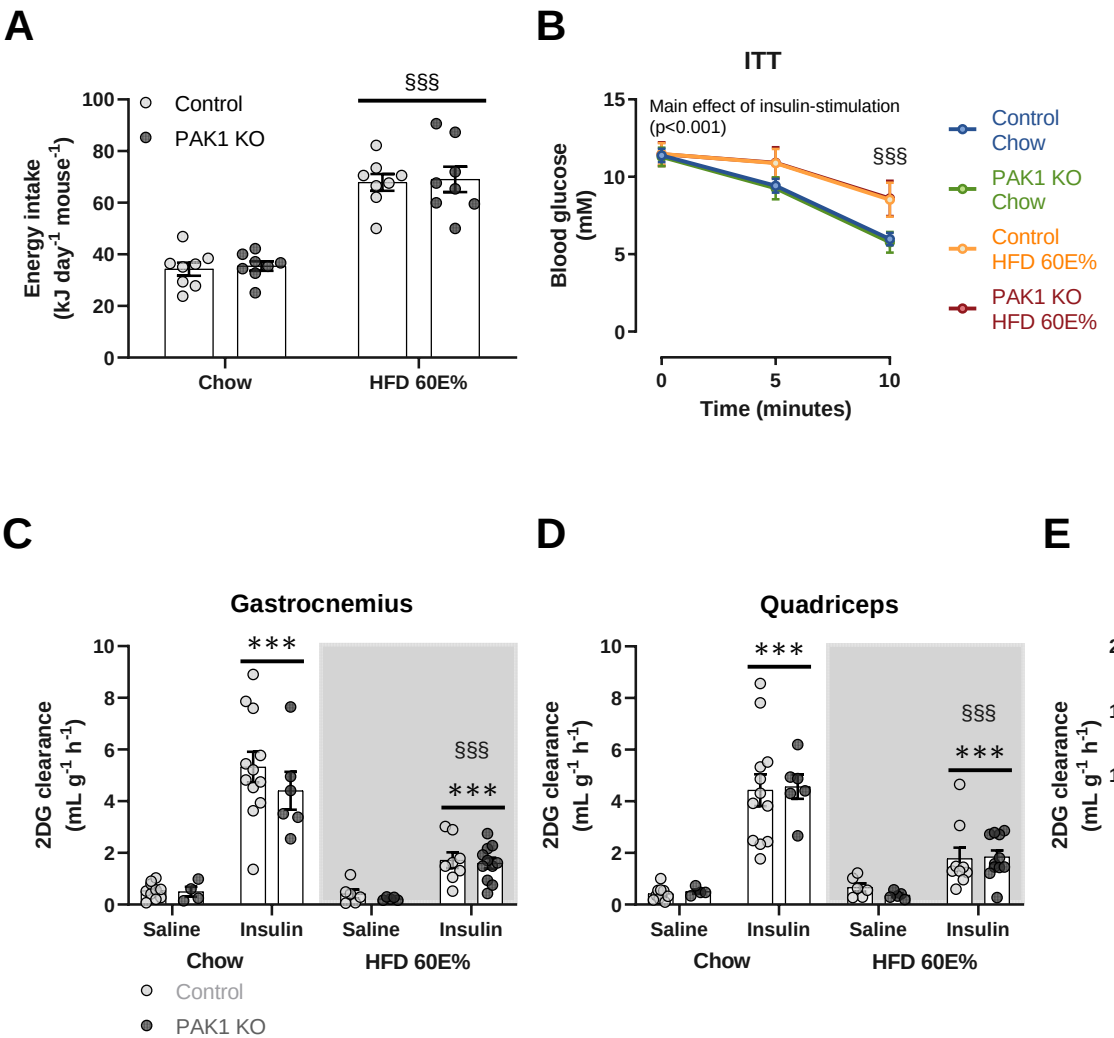

Supplemental figure 2

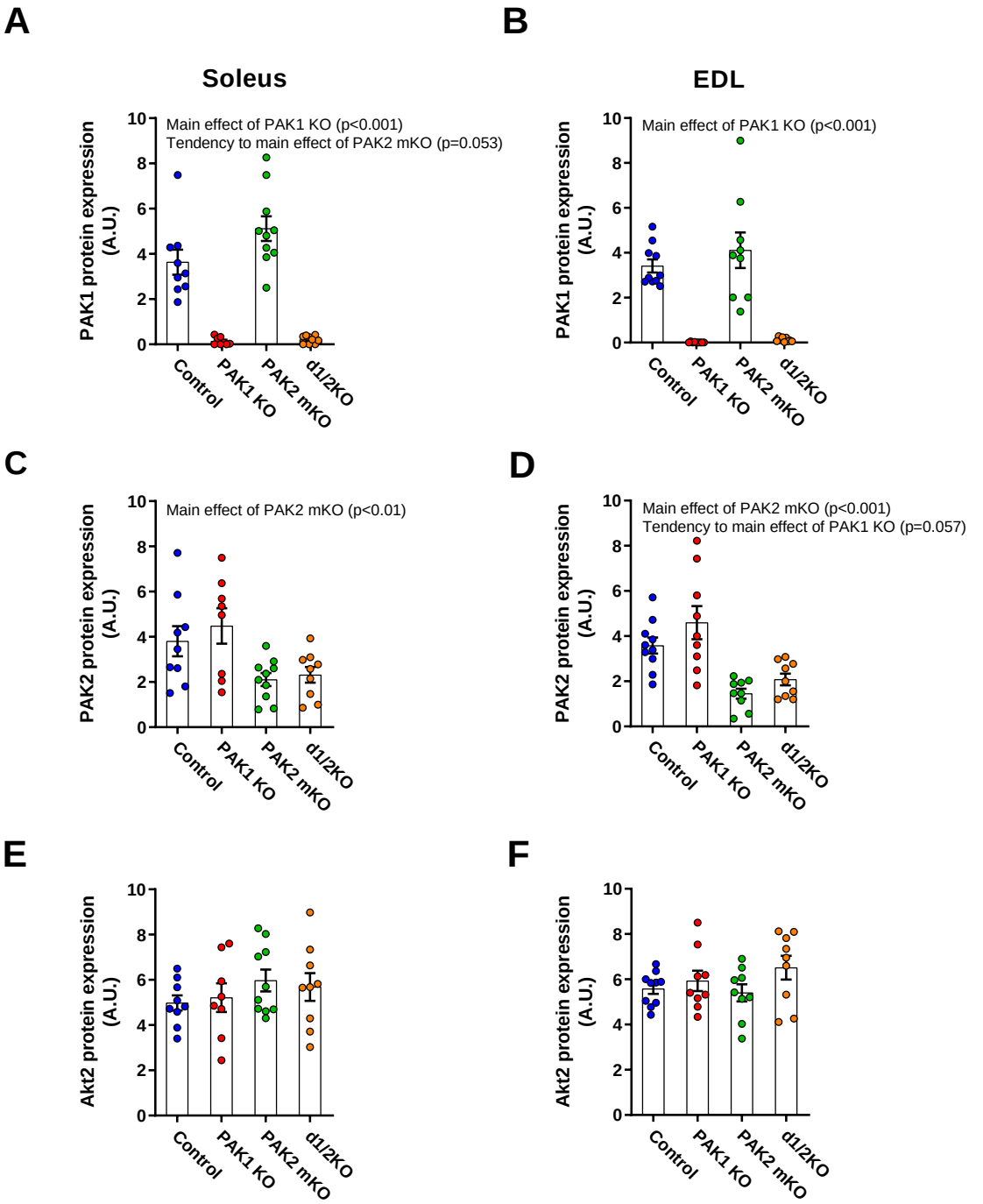

Table 1. Antibody Table

Antibody name	Antibody ID (RRID)	Manufacturer; Catalog Number;	Species Raised in; Monoclonal or Polyclonal
Anti-ACC1, phospho (s79)/ACC2, phospho (S212) Antibody	AB_330337	Cell Signaling Technology; 3661	Rabbit; Polyclonal antibody
Anti-Actin Antibody	AB_476693	Sigma-Aldrich; A2066	Rabbit; Polyclonal antibody
Anti-Akt2 Antibody	AB_2225186	Cell Signaling Technology; 3063	Rabbit, Monoclonal antibody
Anti-Akt, phospho (S473) Antibody	AB_329825	Cell Signaling Technology; 9271	Rabbit; Polyclonal antibody
Anti-Akt, phospho (T308) Antibody	AB_329828	Cell Signaling Technology; 9275	Rabbit; Polyclonal antibody
Anti-AMPK, phospho (T172)	AB_330330	Cell Signaling Technology; 2531	Rabbit, Polyclonal antibody
Anti-GLUT4 Antibody	AB_2191454	Thermo Fisher Scientific; PA1-1065	Rabbit; Polyclonal antibody
Anti-PAK1 Antibody	AB_330222	Cell Signaling Technology; 2602	Rabbit; Polyclonal antibody
Anti-PAK2 Antibody	AB_2283388	Cell Signaling Technology; 2608	Rabbit; Polyclonal antibody
Anti-PAK1, phospho (T423) / PAK2, phospho (T402) Antibody	AB_330220	Cell Signaling Technology; 2601	Rabbit; Polyclonal antibody
Anti-TBC1D4	AB_492639	Millipore; 07-741	Rabbit; Polyclonal antibody
Anti-TBC1D4, phopsho (T642) Antibody	AB_2651042	Cell Signaling Technology; 8881	Rabbit; Monoclonal antibody